

Performance of an exhaled nitric oxide and carbon dioxide sensor using quantum cascade laser-based integrated cavity output spectroscopy

Matthew R. McCurdy

Rice University
Rice Quantum Institute
6100 Main Street
Houston, Texas 77005
and

Baylor College of Medicine
Medical Scientist Training Program
1 Baylor Plaza
Houston, Texas 77030

Yury Bakhirkin
Gerard Wysocki
Frank K. Tittel

Rice University
Rice Quantum Institute
6100 Main Street
Houston, Texas 77005

Abstract. Exhaled nitric oxide (NO) is an important biomarker in asthma and other respiratory disorders. The optical performance of a NO/CO₂ sensor employing integrated cavity output spectroscopy (ICOS) with a quantum cascade laser operating at 5.22 μm capable of real-time NO and CO₂ measurements in a single breath cycle is reported. A NO noise-equivalent concentration of 0.4 ppb within a 1-sec integration time is achieved. The off-axis ICOS sensor performance is compared to a chemiluminescent NO analyzer and a non-dispersive infrared (NDIR) CO₂ absorption capnograph. Differences between the gas analyzers are assessed by the Bland-Altman method to estimate the expected variability between the gas sensors. The off-axis ICOS sensor measurements are in good agreement with the data acquired with the two commercial gas analyzers. This work demonstrates the performance characteristics and merits of mid-infrared spectroscopy for exhaled breath analysis. © 2007 Society of Photo-Optical Instrumentation Engineers. [DOI: 10.1117/1.2747608]

Keywords: breath analysis; nitric oxide; carbon dioxide; integrated cavity output spectroscopy; chemiluminescence; quantum cascade laser.

Paper 06361RR received Dec. 9, 2006; revised manuscript received Feb. 24, 2007; accepted for publication Feb. 26, 2007; published online Jun. 11, 2007.

1 Introduction

The presence of endogenous nitric oxide (NO) in exhaled breath of humans and animals was first reported in 1991.¹ Since then, with more than 1000 publications in the field, it is becoming increasingly apparent that measurements of exhaled NO constitute a new way to monitor the inflammatory status in respiratory disorders, such as asthma and other pulmonary conditions. Exhaled nitric oxide as a measure of inflammation is suggested as providing the best combination of disease evaluation and practical implementation for improved asthma outcomes.² Exhaled nitric oxide has been successfully employed in chronic asthma treatment monitoring to reduce the dose of inhaled corticosteroids, which have serious side effects, without compromising asthma control.³ In treating asthma, which affects 19 million Americans, exhaled NO may soon be incorporated into routine clinical care.⁴

Exhaled NO concentrations from the lower respiratory tract exhibit significant expiratory flow rate dependence.⁵ Because of this, exhaled NO is commonly collected using a single breath maneuver at a constant exhalation flow rate. Exhaled NO sharply rises and reaches a plateau, which can have a positive, negative, or near-zero slope. The plateau concentration is defined as the average concentration over a 3-sec window in the plateau region.⁶ The plateau level is reported as the exhaled NO value. Measurements of the NO plateau at multiple flow rates allow for determination of the origin of

NO (proximal or distal lung) by estimating the flow-independent exchange parameters.⁷

Both offline and online techniques are used to study exhaled NO. In offline sampling, a portion of the exhaled breath is collected in a suitable reservoir for subsequent analysis. In online sampling, NO is measured over time during exhalation. Offline sampling has the advantages of remote collection, independence from instrument response time, and more efficient use of the analyzer, because breath from several patients may be rapidly analyzed in succession. Online sampling has the advantages of immediate identification of contamination from gas not derived from the lower airways, near-instantaneous test results, and no error introduced by sample storage and handling. Online NO analysis is generally preferred for the rapid test result. In both on- and offline collection, breath samples are typically collected at a standardized flow rate using a single exhalation.⁶ Sampling during tidal breath, either spontaneous or paced, is gaining momentum as a noninvasive assessment of lung inflammation in infants and children less than 5 years of age.^{8,9}

The American Thoracic Society and European Respiratory Society (ATS) jointly published requirements for a nitric oxide analyzer.⁶ According to the requirements, a NO analyzer should have a sensitivity of <1 ppbv with a response time of <0.5 sec. Plateau NO measurements during tidal breathing range from 1 to 10 ppb and occur over a short time (<0.5 sec) at the end of a tidal exhalation.^{8,9} Therefore, investigations of NO measurements during tidal breathing require a

Address all correspondence to Frank K. Tittel, Rice Quantum Institute, Rice University, 6100 Main Street - Houston, TX 77005 United States of America; Tel: 713-348-4833; Fax: 713-348-5686; E-mail: fkt@rice.edu

Table 1 Performance summary of five exhaled nitric oxide measurement techniques.

Sensor characteristics	ATS required specifications	Chemiluminescence	Electro-chemical	REMPI TOF-MS	Mid-IR multipass cell	ICOS
Sensitivity	1 ppb	<1 ppb	5 ppb	<1 ppb	<1 ppb	<1 ppb
Response time	<0.5 sec	<0.1 sec	<2 min (total measurement time)	<1 sec	<1 sec	<1 sec
Calibration		Every 14 days or when restarted	Not required	External calibration standard	Not required	Internal

NO sensor with a <0.2-sec response time and an equal or better sensitivity than is required for sampling during a single breath maneuver.

Simultaneous measurement of the exhaled CO₂ profile can be used as a marker of end-exhaled air when collecting breath from mechanically ventilated patients and subjects who are breathing normally.¹⁰ A rapid rise in the inspiratory flow rate and a sharp decrease in end-tidal CO₂ concentrations can be used to adjust and synchronize the NO and CO₂ waveforms both during recording and data processing after NO and CO₂ measurements.¹¹ Additionally, end-tidal CO₂ may be useful as an internal standard to verify correct breath collection and as a normalization procedure to reduce variation in calculating exhaled NO values, as proposed by Roller et al.¹² This technique was used to measure exhaled NO in a diverse population.¹³

2 Available Technologies for Exhaled Nitric Oxide Detection

Several technologies for exhaled nitric oxide measurement have been reported and are summarized in Table 1. In electrochemical analysis, a voltage potential is applied across two electrodes. NO sensing is achieved through oxidation of NO at the electrode surface and measuring the resulting current between the electrodes. Recently, a portable electrochemical analyzer was introduced¹⁴ and compared to chemiluminescence analyzers described later.^{15,16} The electrochemical analyzer showed good agreement with the chemiluminescent analyzer in both studies. However, the 5-ppb sensitivity of the electrochemical analyzer prevents its use in determining the flow-independent NO exchange parameters and for NO concentration measurement during spontaneous breathing.

Mass spectrometry relies on the nonselective ionization of molecules within a sample, requiring a mass-selective apparatus to enhance selectivity. One selective ionization technique is resonance-enhanced multiphoton ionization (REMPI). In this technique, a target species is photoionized and detected using time-of-flight mass spectrometry (TOF-MS). Recently, a system combining REMPI with TOF-MS techniques was reported capable of breath NO measurements.¹⁷ Short, Frey, and Berter report sub-ppbv detection sensitivity in less than 1 sec. A merit of this technique, as well as the optical techniques discussed later, is that multiple target gas species can be detected. Another advantage is

the capability to measure concentrations of isotopomers of NO, which may be useful in metabolic studies.

The chemiluminescent technique is based on a gas-phase reaction between NO and ozone (O₃).¹⁸ Oxygen supplied to the instrument is converted to ozone via a high voltage discharge. NO reacts with ozone in a reaction chamber at a pressure of 4 to 7 torr to produce nitrogen dioxide in the excited state, which releases its energy by emitting light in the visible (>600 nm) spectrum. A photomultiplier converts the emitted light to an electrical current. The amount of light produced is proportional to the amount of nitric oxide in the sample. Current clinical and point-of-care chemiluminescent analyzers for exhaled nitric oxide breath analysis are based on instrumentation developed primarily by Aerocrine, Incorporated,¹⁹ (Providence, New Jersey) and Sievers, Limited (GE Analytical Instruments, Boulder, Colorado). The chemiluminescent analyzer used in this work (model 280, Sievers) has a sensitivity of <1 ppb. However, the need for frequent calibration and high voltage operation has impacted the wide-scale use of chemiluminescent instruments for exhaled NO monitoring in clinics.

Optical techniques have been employed for exhaled nitric oxide detection including photoacoustic, laser absorption, and cavity-enhanced spectroscopy. A sensor using photoacoustic spectroscopy was used to detect and quantify NO, but the reported detection sensitivity was ~500 ppb.²⁰ The sensitivity of such a sensor can be improved by use of distributed feedback (DFB)-QC lasers with higher output power, because the photoacoustic signal detected by the microphones is directly proportional to the incident optical power.

Laser absorption spectroscopy allows sensitive, selective, and fast-response NO concentration measurements. For example, a lead salt laser-based system using a multipass cell has achieved a detection sensitivity of 1.5 ppbv with a 4-sec integration time and is commercially available.²¹ More recently, two thermoelectrically cooled continuous-wave (cw) quantum cascade laser (QCL)-based spectrometers, which achieved sub-ppbv detection sensitivities^{22,23} using a multipass cell, were reported. An innovative QCL-based sensor technology that exploits magnetic field modulation in a Faraday rotation configuration²⁴ has been reported, but so far a minimum NO detection limit of 41 ppbv was observed, which can be improved by using a QC laser targeting a rovibrational line in the Q-branch.

Very sensitive trace gas measurements can be performed using cavity ring-down spectroscopy (CRDS). This technique uses a sample cell constructed of two ultra-low-loss dielectric mirrors (with reflectivities of $R > 99.99\%$), which form a high finesse cavity. A CRDS measurement consists of coupling the laser radiation into the high finesse cavity, rapidly switching off the laser source, and measuring the decay rate of the cavity output radiation. The advantages of CRDS are high sensitivity at sub-ppbv levels^{25,26} due to a long effective optical path, immunity to laser power fluctuations, and self calibration. Halmer et al. used a cavity ring-down absorption spectrometer based on a continuous-wave CO laser to achieve a minimum detectable concentration for NO of 0.8 ppb in 1 sec.²⁷

Integrated cavity output spectroscopy (ICOS) is an alternative method, which also takes advantage of a high finesse cavity, but is less technically demanding than CRDS, as it does not require mode matching or high speed signal sampling electronics required for precise ring-down event measurements. In ICOS only the total laser intensity exiting the high finesse cavity is recorded and not its time dependence. Hence this method relies on exciting many cavity modes simultaneously.^{25,28} Additional dithering of one of the cavity mirrors improves the cavity throughput and helps minimizing mode noise in the resulting absorption spectra. Off-axis injection of the laser beam into ICOS cell provides an increase of spectral density of cavity modes and thus further minimizes the mode noise.^{29,30} Several ICOS-based NO detection systems have been reported.³¹⁻³³ A mid-infrared, cw, thermoelectrically cooled, quantum cascade laser³³⁻³⁵ is an ideal spectroscopic source for ICOS-based sensor platforms for medical diagnostics because of its high power (>0.1 W) and narrow laser spectral width (≤ 3 MHz), necessary for efficient coupling of laser radiation into an ICOS cavity. In this work, we used an off-axis ICOS-based sensor employing a 50-cm-long optical cavity. Details of the performance characteristics of the ICOS-based sensor using a quantum cascade laser operating at $5.47 \mu\text{m}$ (1828 cm^{-1}) were reported previously by the authors.³⁶ In this work, a liquid nitrogen cooled quantum cascade laser operating at $5.22 \mu\text{m}$ (1915 cm^{-1}) was used. We report what we believe to be the first quantum cascade laser-based sensor capable of combined tidal NO and CO₂ concentration measurements.

3 Experimental Method

3.1 Gas Analysis

For simultaneous NO and CO₂ analysis, a quantum cascade laser-based sensor system employing a cw, DFB quantum cascade laser operating at $5.22 \mu\text{m}$ (1915 cm^{-1}), and off-axis ICOS was used.³³ The performance of the ICOS sensor was assessed by evaluating the agreement between the ICOS sensor and two commercial gas sensors. NO was measured with a chemiluminescent nitric oxide analyzer (model 280, Sievers). CO₂ was measured with a capnograph (model 8100, Novamatrix), which uses broadband infrared absorption spectroscopy [also referred to as nondispersive infrared absorption (NDIR)].

The ICOS sensor was always calibrated with a reference mixture of 76 ppbv NO in N₂ before analysis of a breath sample. The sample flow rate into the ICOS system was set at

300 mL/min. The scan rate was chosen to be 5.5 kHz. The data acquisition and processing were realized using a National Instruments LabView-based control platform. Concentration measurements were performed by means of a least-squares linear fitting algorithm of a preacquired spectrum of reference gas mixture. This eliminates the need of taking into account changes in optical pathlength in the ICOS QCL-based system, which is necessary to consider during the synthesis of a spectrum using a spectroscopic database.

The Sievers model 280 was calibrated every two weeks with the manufacturer's recommended 45-ppm NO:N₂ calibration gas mixture and daily using air entrained via an NO filter (Sievers Instruments) as an NO-free gas. The Sievers was calibrated with the NO-free gas more frequently than specified by the manufacturer and at least 20 min were allowed to pass between the 45-ppm gas calibration and sample analysis or NO-free gas calibration to achieve the best accuracy with the chemiluminescent technique. Based on the results of the two previous studies showing the importance of calibration with a low concentration NO gas standard, the chemiluminescent analyzer was calibrated daily with a low concentration (76-ppb NO in N₂) gas mixture.^{37,38} The sample flow rate into the Sievers NO analyzer was 200 mL/min. The NDIR capnograph was also calibrated daily according to the manufacturer's instructions by inserting reference and zero-gas cells provided by the manufacturer into the infrared beam path. The calibration was performed automatically by the capnograph software.

3.2 Breath Collection

A custom-built breath-collection device was used to perform exhaled breath measurements.³⁶ The apparatus meets the American Thoracic Guidelines⁶ for collecting breath for lower airway NO measurement by: 1. providing a back pressure >6 Torr to prevent nasal contamination, and 2. allowing the subject to maintain a constant exhalation flow for online collection. Mouth pressure was maintained by an adjustable stopcock valve and was monitored with a pressure sensor (model 860, Autotran). A constant exhalation flow rate was maintained using feedback from an in-line mass flowmeter (model 4021, TSI Incorporated) displayed on a laptop personal computer (PC) using a Labview interface. The exhalation flow rates ranged from 0.5 to 15 L/min to provide a range of NO concentrations in the breath samples. Only one sample was collected at each flow rate from each subject. For offline collection, the plateau region was determined by first obtaining online NO profiles at each flow rate for each patient and estimating the plateau region based on the exhalation time for each flow rate. Breath was collected at least 2 sec after the estimated start of the plateau region.

3.3 Study Subjects

Subjects were recruited from the Pulmonary Clinic at the Michael E. DeBakey Veterans Affairs Medical Center (MED-VAMC) and from Rice University (Houston, Texas). The breath collection protocol was approved by the Institutional Review Boards of Baylor College of Medicine, MED-VAMC, and Rice University. Written informed consent was obtained from each enrolled patient prior to study entry. The inclusion criteria were age equal to or greater than 21. The exclusion

criteria were the inability to adequately perform the breath collection maneuvers. MED-VAMC patients were included in the study to obtain breath samples from individuals with pulmonary diseases or conditions that alter NO levels (e.g., asthma, chronic obstructive pulmonary disease (COPD), and smoking).

The study subjects were enrolled to obtain biogenic NO in breath samples with varying NO concentrations to compare the NO analyzers. Factors affecting NO such as acute respiratory infection, diet, and medications were not taken into account, since no intra- or intersubject comparisons were made between subjects.

3.4 Offline Nitric Oxide and Carbon Dioxide

Breath samples were collected in 1-L Tedlar bags and measured with both the ICOS sensor and the chemiluminescent sensor. Breath was sampled over a range of exhalation flow rates (from 0.5 to 15 l/min) to produce a range of NO concentrations. To assess the performance agreement of the three sensors, a statistical analysis was employed. We selected the Bland-Altman method³⁹ rather than the Pearson product-moment correlation coefficient. The Pearson product-moment correlation coefficient, as an estimate of agreement between two techniques, can be misleading for several reasons^{39,40}: 1. two sets of data can have high correlation if the points lie along any straight line, not only unity; 2. correlation depends on the range of values; and 3. data with limited agreement can have high correlations. For the Bland-Altman method, a plot of the difference between a pair of measurements (in this case ICOS minus chemiluminescence and ICOS minus NDIR) versus their average is obtained. Subsequently, the limits of agreement between each pair of gas sensors can be determined as differences within ± 2 standard deviations, provided that differences in this range are not clinically important.

Offline CO₂ measurements were made from the same 1-L Tedlar bags used in the previously mentioned offline NO concentration measurements. 28 breath samples were analyzed with the QCL-based ICOS sensor and the capnograph. The ICOS sensor was calibrated with a reference mixture of 5% CO₂ in N₂ after analysis of five samples. The capnograph was calibrated using a reference cell at the start of each measurement session, as recommended by the manufacturer. The limits of agreement were determined using the Bland-Altman method.

3.5 Online and Tidal Nitric Oxide and Carbon Dioxide

For online exhaled breath measurements, a single subject performed single breath maneuvers at six flow rates—0.5, 2, 3, 6, 9, and 15 l/min. As mentioned previously, measurement of the NO plateau for multiple flow rates allows an estimation of flow independent parameters, which may provide additional clinical insight as to the NO output from the alveolar and airway regions of the lung.⁷ Exhaled breath samples were measured by only one instrument, since the sensors were in two different geographic locations and could not be relocated. NO measurements were made using the ICOS sensor and the chemiluminescent sensor. CO₂ measurements were made using the ICOS sensor and the NDIR capnograph. The average and standard deviation of the NO plateau and end-tidal CO₂

were determined for each set of exhaled breaths at each flow rate. For tidal measurements, the flow restrictor was removed from the breathing circuit to allow comfortable spontaneous breathing.

4 Results

4.1 Study Subjects

Study subjects ranged from 29 to 72 years of age. The subject group included five healthy subjects, three patients with asthma, 14 exsmokers with chronic obstructive pulmonary disease, and eight current smokers with chronic obstructive pulmonary disease.

4.2 Offline Nitric Oxide and Carbon Dioxide Comparison

72 breath samples were measured first with the ICOS-based NO sensor followed by the chemiluminescent analyzer, and 65 breath samples were measured in the reverse order, with several hours lapsing between measurements. For exhaled NO, no change in agreement of the results obtained with different sensors was noted during the entire period of this study. Offline NO measurements were performed with a 1.8-sec integration time with both NO sensors. The best to-date minimum detectable NO concentration achieved with the ICOS sensor is 0.4 ppbv with a 1-sec integration time, as determined by 1σ of the Voigt fit residual using a 76-ppb NO calibration gas in N₂ as a balance gas. The average difference in NO concentration measurements between the ICOS and chemiluminescent analyzers (ICOS minus chemiluminescence) was -0.3 ppbv, and the limits of agreement (as $\pm 2\sigma$) were -4.7 and 4.3 ppbv NO. It was observed that the NO concentration gradually decreases with time in the collected breath samples. To remove systematic errors, the offline NO measurements were separated into two groups—those measured with ICOS and then chemiluminescence, and those measured in the reverse order. Figure 1 shows Bland-Altman plots for offline NO concentration measurements for the sequence of ICOS followed by chemiluminescence [Fig. 1(a)] and chemiluminescence followed by ICOS [Fig. 1(b)]. NO concentration measurements from samples measured by ICOS first had an average difference (ICOS minus chemiluminescence) of 1.1 ppb and limits of precision of $\pm \sim 2.9$ ppb (-1.2 - and 4 -ppb NO). NO concentration measurements from samples measured by the chemiluminescent analyzer first had an average difference (ICOS minus chemiluminescence) of -0.7 ppb and limits of precision of $\pm \sim 2.9$ ppb (-3.6 - and 2.1 -ppb NO).

For exhaled CO₂, 28 breath samples were collected during a period of two weeks. Offline CO₂ measurements were made using a 1-sec averaging time. The average difference between ICOS and NDIR shown in Fig. 2 was 0.01 % CO₂, and the limits of agreement were -0.12 and 0.14 % CO₂.

4.3 Online Nitric Oxide and Carbon Dioxide Comparison

Figure 3 shows exhaled NO at 3 l/min measured with ICOS with a 2.4-sec averaging time and computation time, and chemiluminescence with a 2.4-sec averaging time. The solid line represents the average of 15 breath measurements with

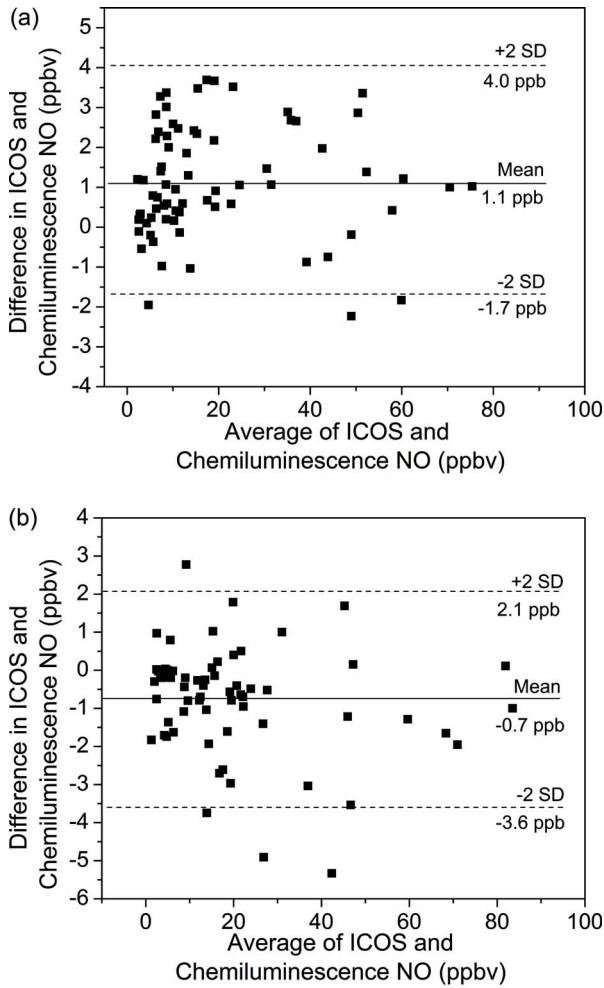


Fig. 1 Bland-Altman plots comparing ICOS and chemiluminescence for offline NO analysis. Each data point represents a pair of measurements plotted as the difference between measurements versus their average. (a) 72 offline NO samples measured with ICOS then chemiluminescence. *Solid line* represents the mean difference between values (ICOS minus chemiluminescence) obtained using the two methods (1.1-ppbv NO). *Dashed lines* represent the limits of agreement, -1.7- and 4-ppbv NO; SD is standard deviation. (b) 65 offline NO samples measured with chemiluminescence then ICOS, with a mean of difference of -0.7 ppbv and limits of agreement -2.1- and 3.6-ppbv NO.

the chemiluminescent analyzer at a 16 samples/sec rate after applying a 50-point Savitzky-Golay smoothing routine with a first-order polynomial. The squares represent the average NO concentration measured by the chemiluminescent analyzer after a 2.4-sec averaging (wide cap error bars are 1 standard deviation for the 15 chemiluminescent breath measurements). The solid circles connected with a dashed line represent average NO measurements with ICOS using a 2.4-sec averaging and computation time (narrow cap error bars are 1 standard deviation for the 15 ICOS breath measurements).

The end-tidal CO₂ did not vary significantly with exhalation flow rate. The standard deviation of end-tidal CO₂ values was equivalent between sensors ($\sigma=0.2\%$ CO₂ for ICOS and NDIR). Figure 4 shows exhaled CO₂ at 2 l/min measured with off axis ICOS (1.8-sec data averaging and computation

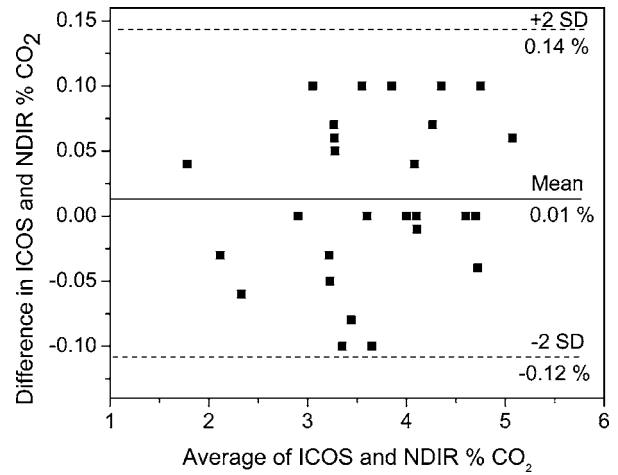


Fig. 2 Bland-Altman plot comparing ICOS and NDIR for offline CO₂ analysis. Each data point represents a pair of measurements plotted as the difference between measurements versus their average. *Solid line* represents the mean difference between values obtained using the two methods (0.01 % CO₂); *dashed lines* represent the limits of agreement, -0.12 % CO₂ and 0.14 % CO₂; and SD is standard deviation.

time) [Fig. 4(a)] and NDIR (1.8-sec data averaging) [Fig. 4(b)]. A time delay between the start of the NDIR CO₂ waveform and the ICOS waveform was observed for all exhalation flow rates.

4.4 Tidal Nitric Oxide and Carbon Dioxide Comparison

An NO waveform was obtained with both the ICOS and chemiluminescence analyzers. Figure 5 shows exhaled NO data collected from the ICOS with a 0.33-sec data averaging

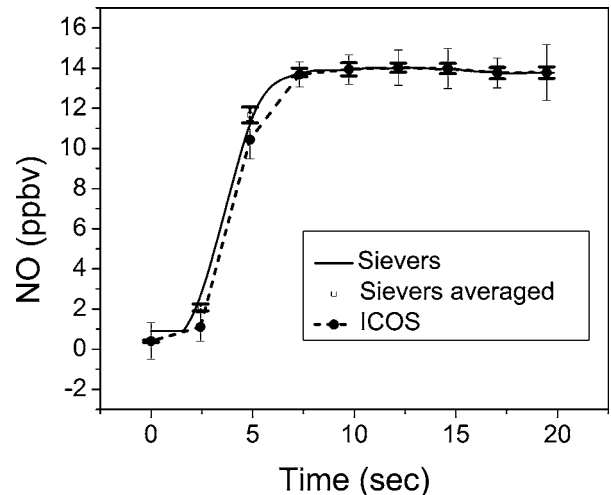


Fig. 3 Online nitric oxide concentrations at 3-l/min exhalation as a function of time. 15 exhaled breaths were measured online with (a) ICOS and (b) chemiluminescence each with 2.4-sec averaging/computation time. *Solid line* represents Sievers data (16 samples/sec) smoothed with a 50 point first-order Savitzky-Golay routine. *Squares with large cap error bars* represent Sievers data after 2.4-sec averaging; *circles with dashed line and small cap error bars* represent ICOS data after 2.4-sec averaging and computation; and error bars are ± 1 standard deviation.

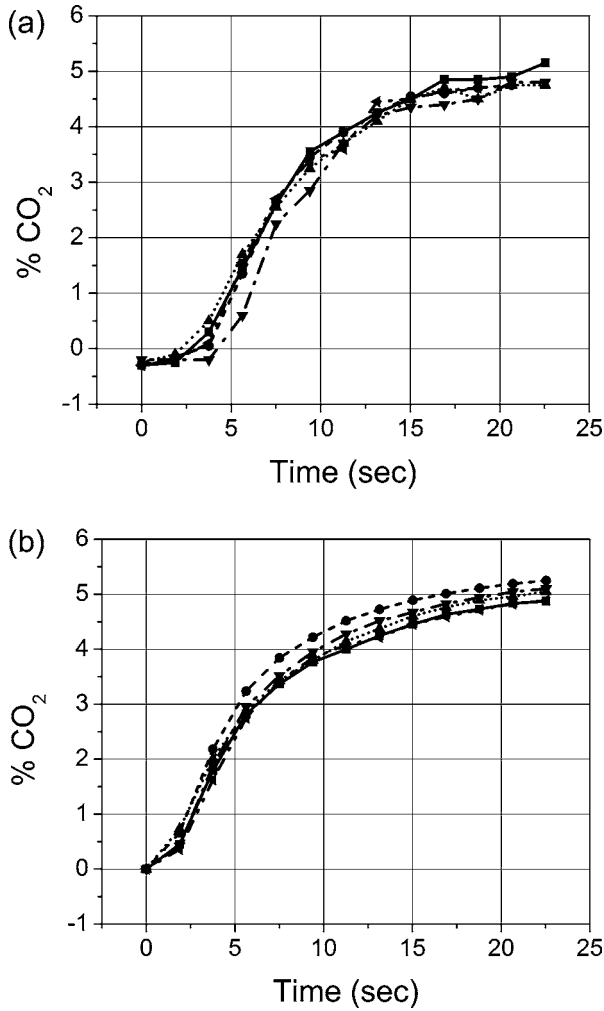


Fig. 4 Online % CO₂ at a 2-l/min exhalation flow rate. Five successive exhaled breaths were measured online with (a) ICOS and (b) a nondispersive infrared (NDIR) capnograph each with a 1.8-sec averaging time.

and computation (3 samples/sec) [Fig. 5(a)] and chemiluminescence with a 16 samples/sec rate during tidal breathing [Fig. 5(b)]. The chemiluminescent data were not averaged to preserve rapid changes in NO over time. For tidal CO₂, the in-line NDIR capnograph detected rapid changes in CO₂, whereas the ICOS sensor had a response delay due to sample cell filling. Figures 6(a) and 6(b) show exhaled CO₂ data collected from the ICOS (0.15-sec averaging and computation) and NDIR (0.15-sec averaging time), respectively. The NDIR capnograph sensor measured a typical expiratory CO₂ waveform⁴¹ consisting of three phases: phase 1, a portion of zero CO₂; phase 2, a rapid rise in CO₂; and phase 3, a plateau region with a small positive slope. The ICOS sensor measured a ramp waveform with end-tidal CO₂ values in agreement with NDIR. Due to the slower gas delivery system, the standard CO₂ phases visible in the waveform acquired by the NDIR capnograph were strongly distorted in the ICOS tidal CO₂ waveform.

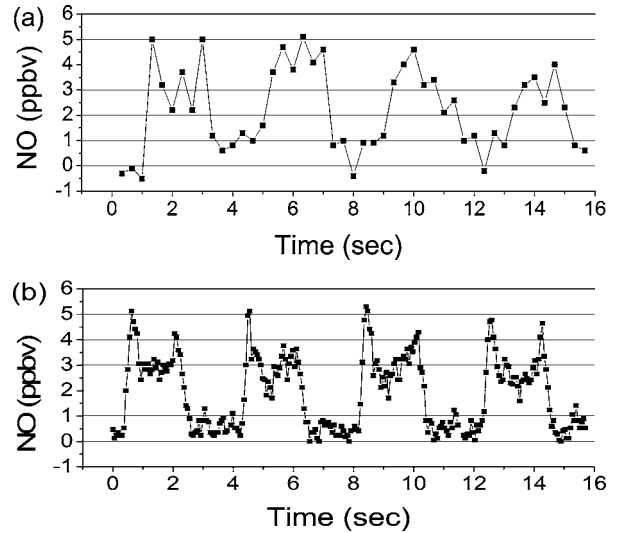


Fig. 5 Exhaled nitric oxide during normal tidal breathing measured with (a) ICOS (0.33-sec averaging and computation time) and (b) chemiluminescence (0.0625-sec averaging time).

5 Discussion

The ICOS offline measurements of exhaled NO and CO₂ are in good agreement with commercially available sensors. In this work, the current gold standards are the chemiluminescence and NDIR methods. The purpose of the Bland-Altman method is to assess the agreement of two methods, where one method is the clinical gold standard and the true value is not known or cannot be easily determined. The Bland-Altman method does not compare the accuracy of the two methods. Instead, the Bland-Altman method is used to determine if the

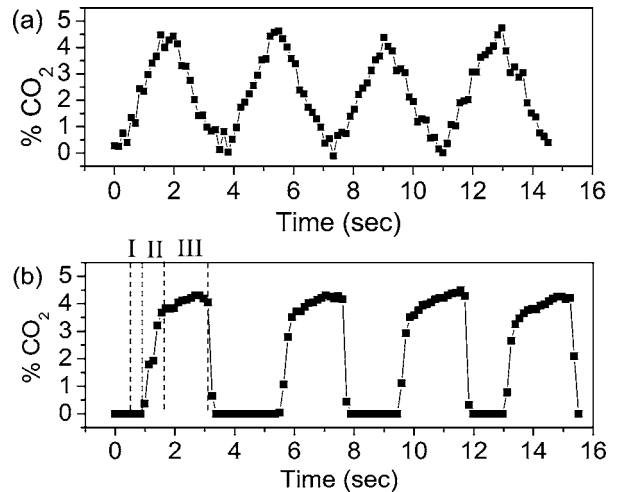


Fig. 6 Exhaled CO₂ during normal tidal breathing measured with (a) ICOS and (b) a nondispersive infrared (NDIR) capnograph using a 0.14-sec averaging time. The three phases of a standard CO₂ expiratory waveform are indicated on the first NDIR expiratory waveform as roman numerals with dashed lines as boundaries. Phase I is the first portion of exhalation with zero CO₂ that occurs ~1 sec after beginning of exhalation; and phase III is the CO₂ plateau region.

new method has readings sufficiently similar to the standard technique to allow the new technique to replace the standard technique in clinical decision making.

For the offline NO concentration measurements, a narrower limit of precision (± 2.9 ppbv) versus the entire dataset (± 4 ppb) was obtained by dividing the offline NO samples into two groups according to the order of analysis: 1. ICOS first and chemiluminescence second, and 2. vice versa. To verify the $2\text{-}\sigma$ limits of precision determined using the Bland Altman method, the standard deviations of both instruments were determined at the time of measurement, which yielded $\sigma = 1.3$ ppbv for the chemiluminescent analyzer and $\sigma = 1.5$ ppbv for the ICOS analyzer. The two standard deviations were added quadratically, yielding 2 ppbv, which is in reasonably good agreement with the $1\text{-}\sigma$ limits of precision (1.5 ppbv) estimated using the Bland-Altman method. The standard deviations of the chemiluminescent and ICOS analyzers were determined using the 76-ppb NO:N₂ calibration gas. The ICOS analyzer was undergoing continuous development during the reported studies, and therefore our best to date minimum detectable NO concentration (0.4 ppbv) was better than the minimum detectable NO concentration measured at the time of intercomparison investigations for the offline measurements.

The limit of precision for each group individually had remarkably similar limits of precision ($\pm \sim 2.9$ ppbv), suggesting that a different systematic error was introduced into each group of data. The systematic error in the offline comparison appeared to be due to a decreasing NO concentration over the 4 to 6 h between consecutive concentration measurements. In the group measured by ICOS first [Fig. 1(a)], the average difference (ICOS minus chemiluminescence) was greater than 0 (1.1 ppbv NO), whereas in the group measured by chemiluminescence first [Fig. 1(b)], the average difference (ICOS minus chemiluminescence) was less than 0 (-0.7 -ppbv NO). This finding suggests that NO is chemically unstable and decreases in Tedlar bags during a 4- to 6-h period.

The ICOS offline CO₂ measurements were in good agreement with the NDIR capnograph. The average difference was 0.01 % CO₂ and the limits of agreement were $+/-0.13$ % CO₂. The percent CO₂ differences are not large enough to be clinically important, and ICOS CO₂ measurements can be used clinically.

For online analysis, the NO plateau concentrations were estimated for breath measurements with both the ICOS and chemiluminescent analyzers over a range of exhalation flow rates (data not shown). The average of 15 NO concentration profiles at a 3 l/min exhalation rate are shown in Fig. 3. The 3-l/min exhalation flow rate was chosen, as it is recommended by the lower airway NO guidelines.⁶ The NO plateau regions for ICOS and chemiluminescence were in good agreement, with all data points within 1 standard deviation of the 15 measurements. The ICOS measurements had a larger standard deviation for each averaged concentration.

Tidal breath NO measurements require subsecond time resolution (<0.2 sec) with a detection sensitivity of ~ 1 ppbv. From Fig. 5, it is evident that the chemiluminescent sensors had adequate sensitivity to detect the plateau NO from the waveform. For tidal NO measurements, better detec-

tion sensitivity of the ICOS sensor is required to improve clinical decision making.

The ICOS sensor was found to be in good agreement with the NDIR capnograph for online end-tidal CO₂ measurements. End-tidal CO₂ varies with ventilation, where increased ventilation produces a lower end-tidal CO₂. Variation in ventilation was minimized in this study by using paced breathing during online and tidal CO₂ measurements. For online CO₂ measurements, the standard deviation of end-tidal CO₂ values was similar ($\sigma = 0.2\%$ CO₂) for the ICOS and NDIR sensors.

The ICOS online CO₂ waveforms began ~ 2 sec after the NDIR waveforms (see Fig. 4). The delay was due to the difference in the position of the sensor in the breath collection system. The NDIR sensor was positioned near the mouth in-line with the exhalation flow, whereas the ICOS sensor drew air from the exhalation flow into the sensor at a rate of 700 ml/min. The time lag is estimated to be ~ 2.4 sec based on the 700 ml/min sample flow rate, an ~ 7 -ml total gas cell volume (at 40 torr), and a 1.8-sec integration time. A time lag was not observed between the chemiluminescent and ICOS sensors because the chemiluminescent sensor also drew air from the exhalation flow.

As with online CO₂ analysis, the different positions of the NDIR and ICOS sensors accounted for the faster response time of the NDIR sensor. The NDIR sensor was able to rapidly detect changes in CO₂ during tidal breathing, allowing visualization of the three phases of exhaled CO₂, labeled in Fig. 6. The gas handling system of the ICOS sensor did not have sufficient time response to resolve the three phases of expiratory CO₂.⁴¹ The maximum sample flow rate of 0.8 l/min into the ICOS sample cell restricted the system gas exchange capability and was the limiting factor in the time resolution of the CO₂ measurement. At the flow rate of 0.8 l/min, the time required for a complete gas exchange within the sampling cell is 2.5 sec. The volume of the ICOS sensor system includes the sample cell and tubing connecting the breath collection system, the sample cell, and the pump. A higher gas flow and smaller total volume would improve the time response of the ICOS sensor. In the case of breath measurement, in which the expected CO₂ concentrations are at levels between 2 and 5%, it is important that the absorption lines are strong enough to have high signal-to-noise ratio but at the same time are not saturated. In this work we were able to target optimal CO₂ absorption lines in the 1915-cm⁻¹ region that allowed for rapid and sensitive exhaled CO₂ measurements.

Simultaneous NO and CO₂ measurements can be made with the ICOS sensor by measuring the NO absorption line at 1915 cm⁻¹ and the CO₂ absorption line at 1915.57 cm⁻¹, accessible within a single frequency scan of the QCL. The line-width of the CO₂ absorption feature is sufficiently low to prevent spectral interference with the neighboring NO line. No spectral interferences from other molecules are present in this wavelength region.

Several improvements can be made to the ICOS sensor to achieve better sensitivity of exhaled NO during tidal breathing and to improve time resolution of CO₂ measurement during tidal breathing. Mirrors with higher reflectivity are available and would improve the sensitivity of both gases and allow a smaller ICOS gas sample cell to be used. Quantum

cascade lasers are available at 1900 cm^{-1} , where the strongest, interference-free NO line in the R-branch of the fundamental ro-vibrational band is located. The 1900-cm^{-1} line is ~ 1.4 times stronger than the 1915 cm^{-1} line used in this work. Wavelength modulation spectroscopy, where the QCL current is modulated at a high frequency and a lock-in amplifier is used to detect the second harmonic frequency, can also be used to improve the signal-to-noise ratio.⁴² Off-axis ICOS sensors have benefited by applying this technique.^{32,33,43} Furthermore, a concentration determination method applied in this work, based on a fitting of the measurement data with the tabulated reference spectrum, can benefit from faster data acquisition by increasing the number of points per laser frequency scan, and thereby reducing the fitting uncertainty.

6 Summary

In this work an exhaled NO/CO₂ sensor for breath analysis using mid-infrared QCL-based integrated cavity output spectroscopy is compared to a commercial chemiluminescence NO sensor and nondispersive infrared absorption CO₂ sensor. The ICOS sensor shows good agreement with the two commercial sensors using offline, online, and tidal sampling techniques. The ICOS sensor has a noise-equivalent sensitivity (1σ) for NO of 0.4 ppbv with a 1-sec averaging time. Potential improvements to the ICOS sensor include incorporating higher reflectivity mirrors and utilizing the NO absorption line at 1900 cm^{-1} . A key advantage of the ICOS-QCL sensor is its ability to simultaneously detect multiple clinically relevant exhaled molecules, in this case NO and CO₂.

Acknowledgments

This work was supported by the National Aeronautics and Space Administration, National Science Foundation (ERC MIRTHE), and the Welch Foundation. The authors wish to thank Stuart Abramson and David Walding of Texas Children's Hospital (Houston, Texas) for generously allowing the use of the Sievers model 280 and Novamatrix model 8100.

References

1. L. E. Gustafsson, A. M. Leone, M. G. Persson, N. P. Wiklund, and S. Moncada, "Endogenous nitric oxide is present in the exhaled air of rabbits, guinea pigs and humans," *Biochem. Biophys. Res. Commun.* **181**, 852–857 (1991).
2. D. Bukstein, M. Kraft, A. H. Liu, and S. P. Peters, "Asthma endpoints and outcomes: What have we learned?" *J. Allergy Clin. Immunol.* **118**, S1–S15 (2006).
3. A. D. Smith, J. O. Cowan, K. P. Brassett, G. P. Herbison, and D. R. Taylor, "Use of exhaled nitric oxide measurements to guide treatment in chronic asthma," *N. Engl. J. Med.* **352**, 2163–2173 (2005).
4. D. R. Taylor, M. W. Pijnenburg, A. D. Smith, and J. C. De Jongste, "Exhaled nitric oxide measurements: clinical application and interpretation," *Thorax* **61**, 817–827 (2006).
5. P. E. Silkoff, P. A. McClean, A. S. Slutsky, H. G. Furlott, E. Hoffstein, S. Wakita, K. R. Chapman, J. P. Szalai, and N. Zamel, "Marked flow-dependence of exhaled nitric oxide using a new technique to exclude nasal nitric oxide," *Am. J. Respir. Crit. Care Med.* **155**, 260–267 (1997).
6. American Thoracic Society and European Respiratory Society, "ATS/ERS recommendations for standardized procedures for the online and offline measurement of exhaled lower respiratory nitric oxide and nasal nitric oxide, 2005," *Am. J. Respir. Crit. Care Med.* **171**, 912–930 (2005).
7. S. C. George, M. Hogman, S. Permutt, and P. E. Silkoff, "Modeling pulmonary nitric oxide exchange," *J. Appl. Physiol.* **96**, 831–839 (2004).
8. A. Artlich, B. Jonsson, M. Bhiladvala, P. A. Lonnqvist, and L. E. Gustafsson, "Single breath analysis of endogenous nitric oxide in the newborn," *Biol. Neonate* **79**, 21–26 (2001).
9. E. Baraldi, C. Dario, R. Ongaro, M. Scollo, N. M. Azzolin, N. Panza, N. Paganini, and F. Zacchello, "Exhaled nitric oxide concentrations during treatment of wheezing exacerbation in infants and young children," *Am. J. Respir. Crit. Care Med.* **159**, 1284–1288 (1999).
10. T. Birken, J. Schubert, W. Miekisch, and G. Noldge-Schomburg, "A novel visually CO₂ controlled alveolar breath sampling technique," *Technol. Health Care* **14**, 499–506 (2006).
11. G. L. Hall, B. Reinmann, J. H. Wildhaber, and U. Frey, "Tidal exhaled nitric oxide in healthy, unexposed newborn infants with prenatal tobacco exposure," *J. Appl. Physiol.* **92**, 59–66 (2002).
12. C. B. Roller, K. Namjou, J. D. Jeffers, W. Potter, P. J. McCann, and J. Grego, "Simultaneous NO and CO₂ measurement in human breath with a single IV-VI mid-infrared laser," *Opt. Lett.* **27**, 107–109 (2002).
13. K. Namjou, C. B. Roller, T. E. Reich, J. D. Jeffers, G. L. McMillen, P. J. McCann, and M. A. Camp, "Determination of exhaled nitric oxide distributions in a diverse sample population using tunable diode laser absorption spectroscopy," *Appl. Phys. B* **85**, 427–435 (2006).
14. T. Hemmingsson, D. Linnarsson, and R. Gambert, "Novel hand-held device for exhaled nitric oxide-analysis in research and clinical applications," *J. Clin. Monit. Comput.* **18**, 379–387 (2004).
15. K. Alving, C. Janson, and L. Nordvall, "Performance of a new hand-held device for exhaled nitric oxide measurement in adults and children," *Respir. Res.* **20**, 57–67 (2006).
16. C. McGill, G. Malik, and S. W. Turner, "Validation of a hand-held exhaled nitric oxide analyzer for use in children," *Pediatr. Pulmonol* **41**, 1053–1057 (2006).
17. L. C. Short, R. Frey, and T. Benter, "Real-time analysis of exhaled breath via resonance-enhanced multiphoton ionization-mass spectrometry with a medium pressure laser ionization source: observed nitric oxide profile," *Appl. Spectrosc.* **60**, 217–222 (2006).
18. A. Fontijn, A. Sabadell, and R. Ronco, "Homogenous chemiluminescent measurement of nitric oxide with ozone. Implications for continuous selective monitoring of gaseous air pollutants," *Anal. Chem.* **42**, 575–579 (1970).
19. P. Silkoff, M. Carlson, T. Bourke, R. Katial, E. Ogren, and S. Szefer, "The aerocrine exhaled nitric oxide monitoring system NIOX is cleared by the US Food and Drug Administration for monitoring therapy in asthma," *J. Allergy Clin. Immunol.* **114**, 1241–1256 (2004).
20. A. Elia, P. M. Lugara, and C. Giancaspro, "Photoacoustic detection of nitric oxide by use of a quantum-cascade laser," *Opt. Lett.* **30**, 988–990 (2005).
21. C. B. Roller, K. Namjou, J. D. Jeffers, M. Camp, A. Mock, P. J. McCann, and J. Grego, "Nitric oxide breath testing by tunable-diode laser absorption spectroscopy: application in monitoring respiratory inflammation," *Appl. Opt.* **41**, 6018–6029 (2002).
22. D. D. Nelson, J. B. McManus, S. C. Herndon, J. H. Shorter, M. S. Zahniser, S. Blaser, L. Hvozdar, A. Muller, M. Giovannini, and J. Faist, "Characterization of a near-room-temperature, continuous-wave quantum cascade laser for long-term, unattended monitoring of nitric oxide in the atmosphere," *Opt. Lett.* **31**, 2012–2014 (2006).
23. B. W. M. Moeskops, S. M. Cstescu, and F. J. M. Harren, "Sub-part-per billion monitoring of nitric oxide using wavelength modulation spectroscopy in combination with a thermoelectrically cooled, continuous wave quantum cascade laser," *Opt. Lett.* **31**, 823–825 (2006).
24. H. Ganser, W. Urban, and J. Brown, "The sensitive detection of NO by Faraday modulation spectroscopy with a quantum cascade laser," *Mol. Phys.* **101**, 545–550 (2003).
25. B. A. Paldus and A. A. Kachanov, "An historical overview of cavity-enhanced methods," *Can. J. Phys.* **83**, 975–999 (2005).
26. A. A. Kosterev, A. L. Malinovsky, F. K. Tittel, C. Gmachl, F. Capasso, D. L. Sivco, J. N. Baillargeon, A. L. Hutchinson, and A. Y. Cho, "Cavity ring down spectroscopic detection of nitric oxide with a continuous-wave quantum-cascade laser," *Appl. Opt.* **40**, 5522–5529 (2001).
27. D. Halmer, G. von Basum, M. Horstjann, P. Herring, and M. Murtz, "Time resolved simultaneous detection of (NO)-N-14 and (NO)-N-15 via mid-infrared cavity leak-out spectroscopy," *Isotopes Environ. Health Stud.* **41**, 303–311 (2005).

28. A. O'Keefe, J. J. Scherer, and J. B. Paul, "CW integrated cavity output spectroscopy," *Chem. Phys. Lett.* **307**, 343–349 (1999).
29. J. B. Paul, L. Larson, and J. G. Anderson, "Ultrasensitive absorption spectroscopy with a high-finesse optical cavity and off-axis alignment," *Appl. Opt.* **40**, 4904–4910 (2001).
30. D. S. Baer, J. B. Paul, M. Gupta, and A. O'Keefe, "Sensitive absorption measurements in the near-infrared region using off-axis integrated-cavity-output spectroscopy," *Appl. Phys. B* **75**, 261–265 (2002).
31. M. L. Silva, D. M. Sonnenfroh, D. I. Rosen, M. G. Allen, and A. O'Keefe, "Integrated cavity output spectroscopy measurements of NO levels in breath with a pulsed room-temperature QCL," *Appl. Phys. B* **81**, 705–710 (2004).
32. Y. A. Bakhrkin, A. A. Kosterev, C. Roller, R. F. Curl, and F. K. Tittel, "Mid-infrared quantum cascade laser based off-axis integrated cavity output spectroscopy for biogenic nitric oxide detection," *Appl. Opt.* **43**, 2257–2266 (2004).
33. Y. A. Bakhrkin, A. A. Kosterev, R. F. Curl, F. K. Tittel, D. A. Yarekha, L. Hvozdar, M. Giovannini, and J. Faist, "Sub-ppbv nitric oxide concentration measurements using cw thermoelectrically cooled quantum cascade laser-based integrated cavity output spectroscopy," *Appl. Phys. B* **82**, 149–154 (2006).
34. S. Blaser, D. A. Yarekha, L. Hvozdar, Y. Bonetti, A. Muller, M. Giovannini, and J. Faist, "Room-temperature, continuous-wave, single-mode quantum cascade lasers at $\lambda_{5.4} \mu\text{m}$," *Appl. Phys. Lett.* **86**, 041109 (2005).
35. L. Diehl, D. Bour, S. Corzine, J. Zhu, G. Hofler, M. Loncar, M. Troccoli, and F. Capasso, "High-temperature continuous wave operation of strain-balanced quantum cascade lasers grown by metal organic vapor-phase epitaxy," *Appl. Phys. Lett.* **89**, 081101 (2006).
36. M. R. McCurdy, Y. A. Bakhrkin, and F. K. Tittel, "Quantum cascade laser-based integrated cavity output spectroscopy of exhaled nitric oxide," *Appl. Phys. B* **85**, 445–452 (2006).
37. Z. Borrill, D. Clough, N. Truman, J. Morris, S. Langley, and D. Singh, "A comparison of exhaled nitric oxide measurements performed using three different analysers," *Respir. Med.* **100**, 1392–1396 (2006).
38. K. C. Muller, R. A. Jorres, H. Magnussen, and O. Holz, "Comparison of exhaled nitric oxide analysers," *Respir. Med.* **99**, 631–637 (2005).
39. J. M. Bland and D. G. Altman, "Statistical methods for assessing agreement between two methods of clinical measurement," *Lancet* **8**, 307–310 (1986).
40. J. Ludbrook, "Statistical techniques for comparing measurers and methods of measurement: a critical review," *Clin. Exp. Pharmacol. Physiol.* **29**, 527–536 (2002).
41. C. T. Anderson and P. H. Breen, "Carbon dioxide kinetics and capnography during critical care," *Crit. Care* **4**, 207–215 (2000).
42. J. Reid and D. Labrie, "Second-harmonic detection with tunable iodine lasers—comparison of experiment and theory," *Appl. Phys. B* **26**, 203–210 (1981).
43. A. Zybin, Y. A. Kuritsyn, V. R. Mironenko, and K. Niemax, "Cavity enhanced wavelength modulation spectrometry for application in chemical analysis," *Appl. Phys. B* **78**, 103–109 (2004).